

Using Spatial Light Modulators in MIMO Visible Light Communication Receivers to Dynamically Control the Optical Channel

Jimmy C. Chau
Electrical and Computer
Engineering
Boston University
jchau@bu.edu

Cristian Morales
Electrical and Computer
Engineering
Boston University
crism@bu.edu

Thomas D.C. Little
Electrical and Computer
Engineering
Boston University
tdcl@bu.edu

Abstract

We propose a new MIMO visible light communication (VLC) receiver architecture that can dynamically adjust the optical channel by using a spatial light modulator (SLM). This capability enables the VLC receiver to track moving transmitters to support mobility. We also present operating procedures and control algorithms for this SLM VLC receiver to measure the gain from each transmitter, to configure the SLM, and to track the transmitters as they move relative to the receiver. Through the design of a two-photodetector prototype and simplified models for imaging systems, we demonstrate that the SLM VLC receiver can outperform similar traditional imaging VLC receivers that do not use an SLM, even if the traditional VLC receiver is equipped with more photodetectors.

Categories and Subject Descriptors

B.4.1 [Input/Output and Data Communications]: Data Communications Device; I.4.1 [Image Processing and Computer Vision]: Digitization and Image Capture

General Terms

Algorithms, Design

Keywords

visible light communication (VLC), spatial light modulator (SLM), MIMO, imaging receiver

1 Introduction

Like MIMO radio-frequency (RF) communication systems, visible light communication (VLC) systems can use multiple transmitters and receiver elements to increase the wireless communication capacity. Unlike MIMO RF systems though, the line-of-sight components tend to dominate over the multipath components in MIMO VLC systems [14]. In the absence of significant fading due to random multipath

signal propagation, the channel gain from each transmitter to each receiver element can be approximated as a deterministic function of the relative positions and orientations of the transmitter and receiver (assuming that the line-of-sight is not obstructed).

The deterministic and position-dependent nature of VLC channel gains presents both disadvantages and advantages. On one hand, MIMO VLC systems do not benefit from the rich scattering that provide the well-conditioned channel matrices in MIMO RF communication systems. This problem is illustrated in the work of Zeng et al., which shows that the bit error rate of a non-imaging VLC system becomes unacceptably high whenever the transmitters are positioned symmetrically about the receiver [14].

On the other hand, the negligible random fading yields a more predictable VLC channel. This predictability presents opportunities to deliberately engineer the VLC channel to improve the resulting MIMO channel capacity.

In this paper, we introduce a new MIMO VLC receiver architecture that incorporates a spatial light modulator (SLM). This built-in SLM enables the VLC receiver to dynamically adjust the optical communication channel to better adapt to changing transmitter and receiver positions in a variety of use cases, such as wireless networking for mobile devices and vehicular networks, where the transmitters or receivers may move freely. As a result of this adaptability, the SLM-based MIMO VLC receiver requires fewer photodetectors than traditional MIMO VLC receivers do to achieve the same performance in mobile use cases.

Section 2 presents background information. Section 3 introduces the SLM MIMO VLC receiver and details its operation. Section 4 presents the channel model for the SLM VLC receiver. Section 5 presents the preliminary procedures and algorithms for controlling the proposed receiver. Section 6 compares the performance of the proposed receiver against other imaging VLC receivers. And Section 7 concludes the paper.

2 Background

In the high signal-to-noise ratio (SNR) regime, MIMO communication systems aim to maximize the rank and minimize the condition number of the channel matrix in order to improve the multiplexing capacity gains [10, p. 294–295]. Two general classes of MIMO VLC receivers have

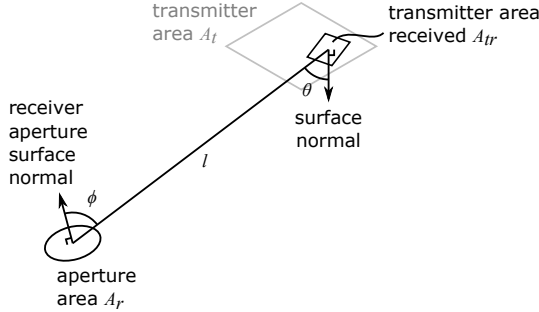


Figure 1. Parameters used in Equation 1 to calculate the gain from a uniformly diffuse transmitter to an imaging receiver pixel.

been previously proposed for this purpose: imaging VLC receivers [14, 1, 3, 13, 2, 7] and non-imaging VLC receivers [11, 6, 12]. Although both types of MIMO VLC receivers can yield full-rank and well-conditioned channel matrices when the transmitters are sufficiently separated from each other, these receivers may yield poorly conditioned channel matrices when the transmitters are close to each other.

For example, the gain from a uniformly diffuse (Lambertian) transmitter to an imaging receiver pixel is

$$\frac{P_r}{P_t} = \frac{A_{tr}A_r}{\pi A_t l^2} \cos \theta \cos \phi \quad (1)$$

where A_r is the area of the imaging receiver's aperture, A_{tr} is the transmitter area seen by the pixel, A_t is the total area of the transmitter's uniformly diffuse emitting surface, l is the distance between the transmitter and the receiver's aperture, θ is the angle between the normal of the transmitter's surface and the straight path from the transmitter to the receiver, ϕ is the angle between the normal of the receiver's aperture and the straight path from the transmitter to the receiver, P_t is the transmitted optical power, and P_r is the received optical power.¹ These parameters are illustrated in Figure 1.

If two transmitters are close enough that their optical signals are entirely received by the same imaging receiver pixels, then the position-dependent parameters (l, θ, ϕ, A_{tr}) would be approximately equal between the two transmitters. Thus, the corresponding columns of the channel matrix would be approximately equal, resulting in a poorly conditioned channel matrix.

In mobile use cases, this situation may arise if the transmitters move near each other or if the receiver is oriented to receive from transmitters that are farther away. Although this problem can be mitigated by increasing the number of pixels in the imaging VLC receiver to reduce the likelihood that signals from neighboring transmitters are received by the same pixels [2], adding additional pixels may require compromises in pixel sensitivity, sampling rate, power consumption, cost, and device size.

Similarly for the non-imaging VLC receivers [11, 6, 12],

¹Derived from [5, ch. 3] assuming only path loss, assuming that neither the transmitter nor the receiver are facing away from each other, assuming no blur in the transmitter's image, and assuming that the transmitters and receivers are small relative to the distance between them.

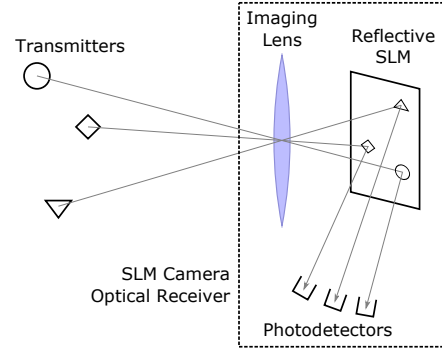


Figure 2. A MIMO VLC system using the SLM Camera Optical Receiver is shown. In this system, an imaging lens focuses light from multiple transmitters onto a reflective SLM that redirects the light from each transmitter to a separate photodetector.

the channel gains to the receiver elements also vary gradually with respect to the relative position and orientation of the transmitters. When the transmitters are positioned close to each other, the corresponding columns of the channel matrix would be similar, resulting in a poorly conditioned channel matrix.

3 Imaging SLM VLC Receiver

The proposed MIMO VLC receiver architecture is an imaging receiver architecture that replaces the traditional image sensor (i.e., photodetector array) with a spatial light modulator (SLM). Unlike traditional imaging receivers, the incoming optical signals are not measured at the image plane (where the images of the transmitters are focused). Rather, an SLM at the image plane redirects the incoming optical signals toward a separate array of photodetectors to be measured.

3.1 Structure of the Receiver

As shown in Figure 2, this SLM Camera Optical Receiver (SLMCOR) architecture consists of an imaging lens, a reflective SLM, and multiple photodetectors; implementations would also require signal-processing and control devices, which are shown in Figure 5. Although a variety of SLMs can be used in imaging SLM VLC receivers, to simplify the description of the architecture, this paper assumes that the SLM is a reflective SLM that consists of a rectangular array of flat micromirrors. Each micromirror can be rotated in place across a range of angles to direct reflected light and each mirror in the array can be independently controlled. By varying the orientation of a pixel's micromirror, the SLM can control the direction that light reflected from that pixel travels², and thus, aim the pixel's light towards a selected photodetector. The photodetectors are arranged around the SLM, facing the SLM, so that each micromirror can redirect light towards any of the photodetectors.

This setup is similar to (and in part, inspired by) the "single-pixel" camera by Duarte et al. [4]. By separating the photodetector(s) from the image plane, the architec-

²For the SLMCOR, "pixel" refers to a single SLM pixel rather than a photodetector because the focused image is formed on the SLM.

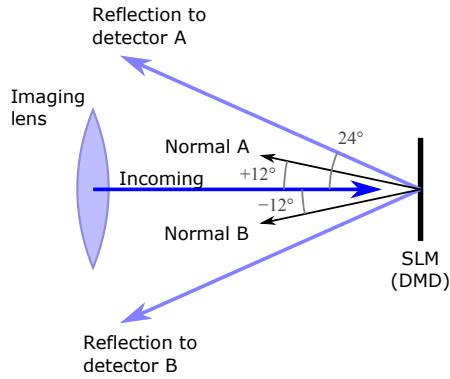


Figure 3. Since each micromirrors can rotate $\pm 12^\circ$, the reflected beam can be deflected by 24° in either direction. The photodetectors should be positioned at $\pm 24^\circ$ to detect the reflected beams.

ture enables the imaging system to have very high resolution with very few photodetectors. This capability allows us to work around the trade-offs described in Section 2 between the quantity of photodetectors and the performance of each photodetector.

Due to the similarity in structure, the SLMCOR can also be used to capture photographs and videos through compressed image sensing as described in [4]. This secondary function may eventually enable the SLMCOR to replace traditional cameras in mobile devices, providing both the capabilities of a camera and a high-speed MIMO VLC receiver in the same device.

Our proposed receiver also differs from the single-pixel camera in significant ways in order to greatly improve the receiver’s sampling rate for high-speed communication signals. One difference is that our receiver uses more than one photodetector—we use one for each transmitter—to sample signals from multiple transmitters simultaneously. Furthermore, as detailed in Section 5, SLMCOR uses different algorithms to generate the SLM patterns by using feedback from the received VLC signals.

3.2 2x2 MIMO SLMCOR Prototype

The SLMCOR was implemented using a Texas Instruments (TI) digital micromirror device (DMD) from the DLP LightCrafter 6500 evaluation kit [8] as the reflective SLM. This DMD has an array of 1920 by 1080 (1080p resolution) micromirrors that are flat in the “reset” state. From this reset state, each micromirror can be independently rotated either $+12^\circ$ or -12° about its diagonal [9]. Since each micromirror can be configured for one of only two possible angles (because pixels cannot be individually placed in the reset/flat position), the micromirrors can be used to switch between two photodetectors. These two photodetectors are positioned at $+24^\circ$ and -24° as explained in Figure 3.

Since each micromirror rotates about its diagonal, we rotated the DMD 45° about its normal vector to align the reflected beams with the photodetectors in the optical-breadboard implementation shown in Figure 4.

As labeled in Figure 4, the DLP-based SLMCOR uses three lenses: one concentrator lens for each photodetec-

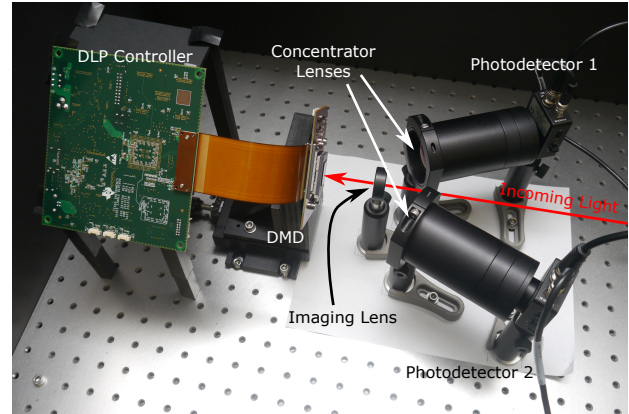


Figure 4. The 2-photodetector SLMCOR prototype using a TI DLP as the SLM.

tor and the main imaging lens. The main imaging lens is a 25.4 mm diameter biconvex lens with a 50.0 mm focal length from Thorlabs (part number LB1471-A). For the DMD’s image area of 14.52 mm by 8.16 mm [9], this relatively long focal length unfortunately yields a relatively narrow field of view (FOV) of approximately $\pm 8.3^\circ$ by $\pm 4.7^\circ$. Although a shorter focal length would provide a wider FOV (enabling the receiver to receive from transmitters in a wider range of positions), we were unable to accommodate a shorter focal length using commercially-available off-the-shelf (COTS) lens holders without obstructing the beams reflected from the DMD. Future revisions of this prototype may be able to improve the FOV, optical gain, and size of the VLC receiver by using custom lenses and optomechanical components.

Another consideration in selecting the main imaging lens was the lens diameter. Although larger lens would enlarge the aperture over which the receiver gathers light, thus improving the receiver’s optical gain, enlarging the aperture would also widen the beam angle of both the light focused onto the DMD and the light reflected from the DMD. Given that the central ray of the reflected beam is offset 24° from the imaging lens’s optical axis, the beam half-angle should not exceed 12° ; otherwise, a portion of the reflected beam would be directed back toward the main imaging lens, where it cannot be detected by a photodetector.

The prototype uses two Thorlabs PDA36A photodetectors. Since the photodetector bodies are relatively large, they are positioned further away from the DMD than the main imaging lens to avoid blocking light from the main imaging lens to the DMD. A Thorlabs LB1723-A 50.8 mm diameter lens is placed in front of each photodetector to focus the reflected beams of light from the DMD onto the photodetector.

Zemax was used to perform ray-tracing simulations to optimize the focus of the lenses and the placement of the components.

4 SLMCOR Channel Model

Applying the small-signal approximation, we make the simplifying assumption that the received shot noise is independent of the transmitted signals. Furthermore, we assume

that each micromirror directs all of its light towards one selected photodetector. Using these assumptions, when the system has n_t transmitters, n_r photodetectors, and n_s SLM pixels, the channel can be modeled as

$$\mathbf{y} = \mathbf{S}(\mathbf{H}\mathbf{x} + \mathbf{w}_s) + \mathbf{w}_t \quad (2)$$

where $\mathbf{x} \in \mathbb{R}^{n_t}$ represents the transmitted signal, $\mathbf{y} \in \mathbb{R}^{n_r}$ represents the received signal, $\mathbf{w}_s \in \mathbb{R}^{n_s}$ represents the shot noise contribution of each SLM pixel (e.g., due to background illumination), $\mathbf{w}_t \in \mathbb{R}^{n_r}$ represents the thermal noise for each photodetector, $\mathbf{H} \in \mathbb{R}^{n_s \times n_t}$ represents the gain from each transmitter through each SLM pixel to a photodetector, and $\mathbf{S} \in \mathbb{R}^{n_r \times n_s}$ represents the fraction of the optical power incident on each SLM pixel that is distributed to each photodetector. For the 2-photodetector DLP-based SLM VLC receiver (2-PD SLMCOR), $n_r = 2$ and $n_s = 1920 * 1080 = 2.0736 * 10^6$.

Effectively, the resulting channel matrix, representing the gain from each transmitter to each photodetector, is

$$\mathbf{G} = \mathbf{S}\mathbf{H} \quad (3)$$

where \mathbf{G} is a n_r by n_t matrix. By controlling the pattern shown by the DMD, the receiver controls \mathbf{S} , and is thus able to adjust the resulting channel matrix.

For the purpose of modeling shot noise (in \mathbf{w}_s), we apply the simplifying assumption that the shot noise variance is identical across all SLM pixels. We further approximate the shot noise, which is actually due to a Poisson process, as additive white Gaussian noise (AWGN).

The elements of \mathbf{w}_t are modeled as independent and identically-distributed AWGN. We neglect other sources of noise.

5 Operation of the 2-PD SLMCOR

In addition to decoding the received signal, SLM VLC receivers also need to configure the SLM to obtain a useful channel matrix. This configuration is orchestrated by the receiver controller using feedback from the received VLC signals as illustrated in Figure 5. For the DMD in the 2-PD SLMCOR, the receiver controller configures the DMD by sending the DLP controller a bitmap image consisting of 1920 by 1080 pixels. Each pixel in the image specifies the orientation of the corresponding micromirror in the DMD: a dark pixel orients the micromirror to direct light towards one photodetector while a bright pixel orients the micromirror to direct light towards the other photodetector. In turn, the DLP controller generates the appropriate electrical signals to move the micromirrors in the DMD. In this paper, we refer to an instance of this SLM configuration as a ‘‘pattern’’.

The generation of SLM patterns can be split into three sub-problems: initially measuring \mathbf{H} , generating the appropriate SLM pattern given \mathbf{H} , and tracking the transmitters as they move relative to the receiver. We present preliminary solutions to these sub-problems for a proof-of-concept. Future strategies will likely further improve the performance of SLM VLC receivers.

5.1 Initially Measuring \mathbf{H}

As explained in Section 4, the resulting channel matrix is determined by both \mathbf{S} and \mathbf{H} . To optimize the channel matrix,

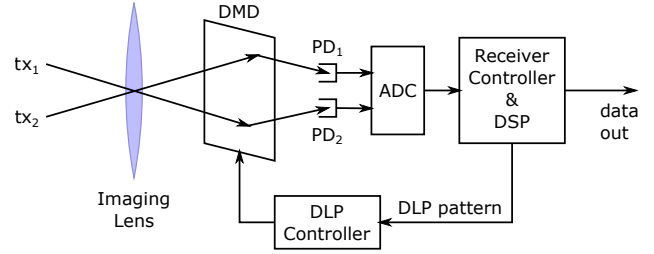


Figure 5. A block diagram of the 2-PD DLP SLM VLC receiver showing the control loop and signal chain.

the receiver controller first measures \mathbf{H} : the gain from each transmitter to a photodetector through each SLM pixel. For simplicity, we assume that this gain is the same for either photodetectors.

To facilitate transmitter-to-photodetector gain measurements, to enable the receiver to identify which transmitter transmitted any signal, and to facilitate the tracking of transmitters as they move relative to the receiver, we propose allocating a small portion of the available bandwidth for each transmitter to embed a continuously-transmitted unique identification signal of a known amplitude. At the receiver, the identification signal can be isolated by filtering to pass the identification band, and (assuming that the gain of the identification signal is representative of the gain at other frequencies) the channel gain (in \mathbf{H}) can be determined by dividing the amplitude of the received identification signal by the amplitude of the transmitted identification signal.

To ensure that the identification signals can be separated from each other in case of interference between multiple transmitters, the unique identification signals should be orthogonal to each other. This orthogonality can be achieved by selecting m_t evenly spaced frequencies within the identification band as the unique identification signals, where m_t is the maximum supported number of active transmitters that can be in the receiver’s field of view. Assuming that \mathbf{H} varies very slowly (compared to the VLC symbol rate), these identification symbols can be sampled over long periods of time, allowing the receiver to finely resolve differences in frequency. As a result, the identification band can have a very narrow bandwidth, and thus, reserving this band for identification and channel-state measurements would not significantly decrease the capacity of the system.

The transmitter-to-photodetector gain through each pixel can be measured by first splitting the pixel array in half, directing half of the pixels toward photodetector 1 (PD1) and the other half toward photodetector 2 (PD2). The signals received by both photodetectors are checked for the presence of any transmitter’s identification signal (that is significantly above the noise floor). If no identification signal is found, then the rows of \mathbf{H} corresponding to those pixels are 0. The process is then repeated recursively for each partition of pixels that do receive an identification signal, splitting the partition in half and using just PD1 to sample one sub-partition at a time (since PD2 must be used to receive from all other pixels), until the partition consists of just one pixel. When the partition consists of just one pixel, the originating transmitter

and gain of the signal that is received by the pixel can be determined by measuring the identification signal as described above.

Future protocols may be able to further reduce the time needed to initially measure \mathbf{H} .

5.2 Generating the SLM Pattern

Given \mathbf{H} , the receiver controller can determine how many active transmitters are in the receiver's field of view and which transmitter images are incident on which SLM pixels.

If only one transmitter is in the FOV, the receiver controller can generate an SLM pattern to remove shot noise from the received VLC signal by directing the VLC signal and background light toward different photodetectors. This can be done by directing background light from the pixels that do not receive from the transmitter toward PD2 while directing the VLC signal from the pixels that do receive from the transmitter toward PD1. In this single-input and multiple-output (SIMO) scenario, the SLMCOR performs selection diversity combining.

If two transmitters are in the FOV, pixels receiving signals from the first transmitter can be directed towards PD1 and pixels receiving signals from the second transmitter can be directed towards PD2. Pixels that receive from both transmitters can be directed based on which transmitter has a greater gain through that pixel. Since every DMD pixel must direct light towards one of the two photodetectors, the remaining pixels that receive no VLC signal and only contribute to shot noise can be directed randomly toward either photodetector.

The 2-PD DLP SLM VLC receiver cannot simultaneously receive from more than two transmitters due to the limited number of photodetectors. However, if more than two transmitters are available, the additional transmitters can each be configured to duplicate one of the two transmitters' signals to improve the received signal strength.

5.3 Tracking the Transmitters

Since the 2-PD DLP SLMCOR requires both photodetectors to receive from any transmitter, the method described in Subsection 5.1 cannot be used to update the measurements of \mathbf{H} (i.e., track the transmitters) while the SLMCOR is receiving any VLC signal. To update a row of \mathbf{H} after initialization, we propose a procedure to perturb the SLM pattern to measure the incremental changes in gain from the transmitters.

First, measure the amplitude of each identification signal received by both photodetectors. Since the identification signals are continuously transmitted and orthogonal to the data portion of the VLC signals, this measurement can be done without interrupting data transmission.

Then, toggle the DMD pixel corresponding to the row of \mathbf{H} to be updated so that the pixel switches from one photodetector to the other. We assume that the resolution is sufficiently high that the VLC signal from any transmitter would land on many pixels, so changing the state of one pixel would not alter the transmitter-to-photodetector gains enough to significantly increase the probability of error.

After toggling the pixel, measure the amplitude of each identification signal received by both photodetectors again.

Table 1. Simulation parameters used for the performance comparison.

Parameter	Value
Aperture radius	25.4 mm
Lens to array distance	49.9 mm
Pixel array width	14.52 mm
Pixel array height	8.16 mm
Receiver position	(0, 0, 0) (imaging lens at origin)
Receiver zenith angle	0° (in the +z-axis direction)
Transmitter shape	40 mm by 40 mm (square)
Transmitter position	$z = 2.5$ m
Transmitter orientation	downward

Assuming that no other event altered the transmitter-to-photodetector gains during this procedure, the change in amplitude of each identification signal is entirely due to the toggled pixel. Thus, the difference in amplitude of each identification signal can be treated as the incremental contribution of the toggled pixel, and can be used to calculate the gains through that pixel by dividing this incremental contribution by the amplitude of the identification signals at the transmitter.

The receiver may prioritize updating the rows of \mathbf{H} that correspond to pixels near the boundaries of the DMD and near the boundaries of transmitter images to better track transmitters as they move incrementally or as they enter the field of view.

6 Performance

We compare the 2-PD SLMCOR against traditional imaging VLC receivers with 2, 4, and 9 photodetectors to illustrate the advantage of the SLMCOR architecture. In this comparison, we simulate each of the receivers with two pseudo-randomly positioned transmitters in the receiver's field of view to determine the average channel matrix rank and median channel matrix condition number. These two metrics (the rank and condition number) indicate the capacity of the MIMO channel in the high SNR regime [10, p. 294–295].³ We use the median condition number instead of the mean condition number as the metric because the condition numbers may be infinite.

To isolate and highlight the effects of adding an SLM, we use the same optical system parameters for both the DLP-based and the traditional imaging VLC receivers. These simulation parameters are chosen to match the SLMCOR prototype described in Subsection 3.2 and are listed in Table 1. For each imaging receiver in the simulations, the pixels are tiled in a rectangular array to cover the entire area of the pixel array without overlap (for a 100% fill factor).

In each of the 1000 trials simulated to obtain the mean rank and median condition number, the centers of the two transmitters are uniformly distributed within the receiver's field of view on the plane at $z = 2.5$ m.

To determine where each transmitter's image lands on the

³Although the RF channel model used in [10] differs in significant ways from VLC channels (e.g., VLC signals are non-negative and may be non-Gaussian), we assume that these metrics remain sufficiently valid for a rough comparison between VLC systems.

Table 2. Simulation results comparing average rank and median condition number of VLC systems using the 2-PD SLMCOR versus using 2-, 4-, or 9-pixel traditional imaging VLC receivers. The standard deviation (SD) of the rank is also shown.

	Average rank	Rank SD	Median condition number
2-PD SLMCOR	2.00	0.00	1.02
2-pixel traditional	1.53	0.50	6.12
4-pixel traditional	1.81	0.40	1.21
9-pixel traditional	1.94	0.24	1.18

receiver's pixel array, we assume that the imaging receiver is perfectly in focus, and apply the paraxial thin-lens approximation. With this simplification, the transmitter image lands where the ray from the transmitter that goes through the center of the imaging lens intersects with the image plane. Conversely, the portion of the transmitter seen by a pixel can be determined by projecting the pixel's polygon through the center of the imaging lens to the transmitter's plane (at $z = 2.5$ m) as illustrated in Figure 1.

Given this projected pixel polygon on the transmitter's plane, Equation 1 can be used to determine the gain from each transmitter to each pixel. A_{tr} can be determined as the area of the intersection between the transmitter polygon and the projected pixel polygon. We assume that each pixel is sufficiently small that l , θ , and ϕ does not vary significantly over the area of the pixel.

The simulation results are highlighted in Table 2. A higher rank and a condition number closer to one indicate better MIMO performance in the high SNR regime. These results show that the 2-photodetector DLP SLM VLC receiver is able to significantly out-perform the traditional imaging VLC receivers, even when the traditional imaging VLC receivers use more photodetectors.

7 Conclusion

MIMO VLC systems differ from MIMO RF systems in significant ways. Due to a lack of multipath signal propagation, VLC channel gains depend strongly on the relative positions of the transmitters with respect to the receiver and do not vary significantly from random fading. As a result, a VLC system may perform poorly whenever the transmitters and receiver are in certain positions; in the absence of random fading over time, these poor channel conditions may persist until the transmitters or receiver moves. These dead spots limit the utility of MIMO VLC systems for mobile use cases.

In this paper, we propose a new MIMO VLC receiver architecture that can dynamically alter the channel matrix using a spatial light modulator to both avoid dead spots and to enhance the performance of the resulting channel. By taking advantage of the relatively slow-changing nature of VLC channel gains, the proposed SLM VLC receiver can measure and adjust the channel matrix to improve SNR and to track transmitters as they move relative to the receiver.

Although the current DLP-based SLM VLC receiver can only support two photodetectors, we demonstrate through simulations that the SLM VLC receiver still outperforms imaging VLC receivers that have more photodetectors in regards to channel matrix rank and condition number. In future work, we aim to increase the number of photodetectors

that can be supported by the SLM VLC receiver, refine our preliminary algorithms for controlling the VLC receiver, validate our simulation results through our physical prototype, and develop better metrics to compare VLC receivers.

8 Acknowledgment

This work was supported primarily by the Engineering Research Centers Program of the National Science Foundation under NSF Cooperative Agreement No. EEC-0812056.

9 References

- [1] A. Azhar, T.-A. Tran, and D. O'Brien. Demonstration of high-speed data transmission using MIMO-OFDM visible light communications. In *GLOBECOM Workshops (GC Wkshps)*, 2010 IEEE, pages 1052–1056, 2010.
- [2] J. C. Chau and T. D. C. Little. Scalable imaging VLC receivers with token-based pixel selection for spatial multiplexing. In *Proceedings of the 1st ACM MobiCom Workshop on Visible Light Communication Systems, VLCS '14*, pages 21–26, New York, NY, USA, 2014. ACM.
- [3] K. Dambul, D. O'Brien, and G. Faulkner. Indoor optical wireless MIMO system with an imaging receiver. *Photonics Technology Letters*, IEEE, 23(2):97–99, Jan. 15, 2011.
- [4] M. Duarte, M. Davenport, D. Takhar, J. Laska, T. Sun, K. Kelly, and R. Baraniuk. Single-pixel imaging via compressive sampling. *Signal Processing Magazine, IEEE*, 25(2):83–91, 2008.
- [5] N. S. Kopeika. *A System Engineering Approach to Imaging*. SPIE Optical Engineering Press, 1998.
- [6] A. Nuwanpriya, S.-W. Ho, and C. S. Chen. Angle diversity receiver for indoor MIMO visible light communications. In *Globecom Workshops (GC Wkshps)*, 2014, pages 444–449, Dec 2014.
- [7] S. Rajbhandari, H. Chun, G. Faulkner, D. O'Brien, A. V. N. Jalajakumari, K. Cameron, R. Henderson, E. Xie, J. J. D. McKendry, J. Hermsdorf, E. Gu, M. D. Dawson, D. Tsonev, M. Ijaz, and H. Haas. Multi-gigabit integrated MIMO visible light communication system: Progress and updates. In *Proceedings of IEEE Photonics Summer Topicals*, pages 230–231, 2015.
- [8] Texas Instruments. *DLP LightCrafter 6500 and 9000 EVM User's Guide*, December 2014. Literature Number: DLPU028A.
- [9] Texas Instruments. *DLP6500FYE DMD*, October 2014. DLPS053.
- [10] D. Tse and P. Viswanath. *Fundamentals of Wireless Communication*. Cambridge University Press, 2005.
- [11] T. Wang and J. Armstrong. Performance of indoor MIMO optical wireless system using linear receiver with prism array. In *Communications Theory Workshop (AusCTW)*, 2014 Australian, pages 51–56, Feb 2014.
- [12] T. Wang, C. He, and J. Armstrong. Angular diversity for indoor MIMO optical wireless communications. In *Communications (ICC)*, 2015 IEEE International Conference on, pages 5066–5071, June 2015.
- [13] T. Q. Wang, Y. A. Sekercioglu, and J. Armstrong. Hemispherical lens based imaging communication MIMO optical wireless communications. In *3rd IEEE Workshop on Optical Wireless Communications (OWC'12)*, pages 1239–1243, Dec 2012.
- [14] L. Zeng, D. O'Brien, H. Minh, G. Faulkner, K. Lee, D. Jung, Y. Oh, and E. T. Won. High data rate multiple input multiple output (MIMO) optical wireless communications using white LED lighting. *Selected Areas in Communications, IEEE Journal on*, 27(9):1654–1662, December 2009.